Indian J. Phys. **73B** (2), 203-214 (1999)

IJP B
an international journal

Electron impact excitation of the n^1P, n^3P, n^1D and n^3D states of Mg(n=3) and Zn(n=4) atoms

Savinder Kaur, Surbhi Verma and Rajesh Srivastava

Department of Physics, University of Roorkee, Roorkee-247 667, Uttar Pradesh, India

Abstract : Distorted-wave approximation calculations have been carried out for electron impact excitation of the $3^{1,3}P$ and $3^{1,3}D$ states of magnesium and $4^{1,3}P$ states of zinc from their respective ground 3^1S_0 and 4^1S_0 states. Results for the differential cross sections, coherence and correlation parameters are obtained and reported at incident electron energies of 20 and 40 eV. The results for magnesium are discussed and compared with other available theoretical and experimental data while the results for the zinc atoms are compared with the only available our earlier relativistic distorted-wave approximation calculations

Keywords : Electron impact excitation, Zn atoms, distorted wave approximation

PACS Nos. 34.80.Dp, 34.80.Nz

1. Introduction

Relatively few earlier experimental and theoretical results have been reported for the electron impact excitations of alkaline earth atoms. However, recent experimental activities in measuring the differential cross sections (DCS) as well as coherence and correlation parameters for the alkaline earth atoms ([1-5] and references cited therein) have renewed interest in similar theoretical work ([6-9] and references therein).

In our previous work [9] we carried out calculations using a fully relativistic distorted wave (RDW) approximation theory for the electron impact $^1S_0 \rightarrow 3^1P_1$, $3^3P_{0,1,2}$, 3^1D_2, $3^3D_{1,2,3}$ excitations in magnesium and $^1S_0 \rightarrow 4^1P_1$, $4^3P_{0,1,2}$ excitations in zinc atoms. In this paper review of all earlier work was given and the RDW results for DCS, coherence and correlation parameters as well as spin polarisation parameters at incident electron energies of 10, 20 and 40 eV were presented. For $3^{1,3}P_J$ excitations in magnesium experimental and some other non-relativistic theoretical calculations using distorted wave and close-coupling approximations were available with which we compared our RDW calculations. While for $3^{1,3}D_J$ excitations in Mg and $4^{1,3}P_J$ excitations in Zn we reported our RDW calculations for the first time and there were no other calculations for comparison.

In the absence of any other theoretical or experimental results for comparison with our RDW results for $4^1S \rightarrow 4^{1,3}P$ excitations in Zn, the main aim of this paper is to carry out a non-relativistic distorted wave approximation (DWA) calculation for Zn and present an inter-comparison to gain confidence of the suitability of the two approximation methods. Further the agreement of the results from the RDW as well as earlier theories with experiment was not very convincing for $3^1S \rightarrow 3^{1,3}P$, $3^{1,3}D$ excitations in Mg. We also take up therefore these excitations in Mg in the present paper and carry out DWA calculations for them. We believe our present study will enable us also to assess the relative contribution of the relativistic effects when we compare the DWA results of this paper with our earlier RDW results. Detailed results are obtained and reported at the incident electron impact energies of 20 and 40 eV (where the DWA is expected to be reliable) for the differential cross sections as well as the coherence and correlation parameters.

2. Theoretical considerations

2.1 Distorted wave approximation theory :

In the first-order distorted wave approximation, the transition matrix for excitation of an atom with N-electrons from an initial state i to any other excited magnetic sub-state f_m can be written as (atomic units are used throughout)

$$T_{if_m} = \langle \chi^-_{f_m} \left| V - U_f(\boldsymbol{r}_{N+1}) \right| \mathcal{A} \chi^+_i \rangle, \tag{1}$$

where $\mathcal{A}$ is the antisymmetrization operator which takes into account in the T-matrix, the effect of electron exchange between projectile and target electrons. V is the total interaction potential given by

$$V = -\frac{Z}{r_{N+1}} + \sum_{i=1}^{N} \frac{1}{\left| \boldsymbol{r}_i - \boldsymbol{r}_{N+1} \right|}. \tag{2}$$

Here Z is the nuclear charge of the target atom, and $\boldsymbol{r}_j$, $\boldsymbol{r}_{N+1}$ are respectively, the position coordinates of the target j-th electron and the projectile electron with respect to nucleus of the target. $\chi^+_i(\chi^-_{f_m})$ is the combined wavefunction of the incident (scattered) electron and target atom in the initial (final) state which can be expressed as

$$\chi^{+(-)}_{i(f_m)} = \phi_{i(f_m)}(\boldsymbol{r}_1, \boldsymbol{r}_2, \ldots, \boldsymbol{r}_N)\, F^{+(-)}(\boldsymbol{k}_{i(f)}, \boldsymbol{r}_{N+1})\, S_{i(f)}(1, 2, \ldots, N; N+1). \tag{3}$$

Here, $\phi_{i(f_m)}$ is the initial (final) target atom wavefunction and $S_{i(f)}$ is the initial (final) channel state spin function for the composite system consisting of the incident projectile and the target. $F^{+(-)}(\boldsymbol{k}_{i(f)}, \boldsymbol{r}_{N+1})$ are the projectile distorted waves with the wave vector $\boldsymbol{k}_{i(f)}$ and satisfy

$$\left[\nabla^2_{N+1} + k^2_{i(f)} - 2U_{i(f)}(\boldsymbol{r}_{N+1})\right] F^{+(-)}(\boldsymbol{k}_{i(f)}, \boldsymbol{r}_{N+1}) = 0. \tag{4}$$

Here +(−) refers the usual in (out) – going boundary condition. The distortion potential $U_{i(f)}$ is given by

$$U_{i(f)} = V_a^{stat} + V_{i(f)}^{ex}, \qquad (\text{with } a = i \text{ or } f) \tag{5}$$

V_a^{stat} is the spherically averaged static potential of the atom in the initial or final state depending on whether a is i or f and obtained from the relation

$$V_a^{stat} = < \phi_a \mid V \mid \phi_a >. \tag{6}$$

$V_{i(f)}^{ex}$ is the exchange distortion potential in the initial (final) channel and is taken to be that from Furness and McCarthy [10].

$$V_{i(f)}^{ex} = \frac{1}{2}\left\{\left(\frac{1}{2}k_{i(f)}^2 - V_a^{stat}\right) - \left[\left(\frac{1}{2}k_{i(f)}^2 - V_a^{stat}\right)^2 - 8\pi\tau\rho_a\right]^{1/2}\right\}. \tag{7}$$

Here, ρ_a is the spherical one electron charge density of the target atom in the initial or final channel depending on whether a is i or f. This is expressed as $\rho_a(r) = \int dr' \left|\phi_a(r,r')\right|^2$. The value of the τ parameter depends on the total spin of the colliding system in the initial and final channel for a particular transition. Following Vucic *et al* [11] for scattering from the target in a triplet state in the doublet (quartet) mode $\tau = -1$ (+2) and for scattering from the target in a singlet state in the doublet mode $\tau = 1$, the above form for $V_{i(f)}^{ex}$ of Furness and McCarthy [10] is infact one of the best local approximations for the exchange potential in the intermediate electron energy region and has been widely used in literature.

Further, in principle, in the DWA the distortion potential $U_{i(f)}$ may be chosen of any mathematical form in any suitable arbitrary manner [12]. However, three choices of the distortion potential have generally been made in the literature. These are such that either the ground state (II) or the excited state (FF) distortion potential is taken in both the initial and final channels, or the distortion of the initial state in the initial channel and the excited state in the final channel (IF) are taken. The IF choice has been frequently adopted earlier which is the traditional distorted wave approach described by Mott and Massey [13]. However, there are a number of DWA calculations which suggest that the use of II and FF model explains the experimental data in a better way and ensure also the orthogonality between the incident and scattered electron distorted waves. However, the reason why these two choices (*viz.* II and FF) should be better is not clear. It is most likely that to some degree it accounts for the missing second or higher order effects in the first order calculation [12, 14]. Keeping in mind the above situation, we have carried out the present calculations in the FF model.

The wavefunctions for n^1S, n^1P, n^3P, n^1D and n^3D states of magnesium ($n = 3$) and zinc ($n = 4$) are obtained using the Hartree-Fock code of Froese Fischer [15]. The distortion potentials are also generated from this code. Further, the excitation scattering amplitude a_m in the "collision reference frame" is related to the DWA transition matrix element T_{if_m} by

$$a_m = -\left(\frac{1}{2\pi}\right) T_{if_m} \tag{8}$$

2.2 *Stokes parameters (P_i, $i = 1$–4) and alignment and orientation parameters :*

The analysis of the polarization of the photon emitted from the excited atom in coincidence with the detection of the scattered electron is carried out in terms of usual differential Stokes

parameters P_i, $i = 1$ to 4. These Stokes parameters thus give the information about the state of the excited atom (*i.e.* relative magnitudes and phases of the different magnetic sublevels).

In order to calculate the Stokes parameters, P_i, $i = 1$ to 4, theoretically, we follow Blum [16] who expressed these in terms of the state multipoles $< T(L)^{+}_{KQ} >$ of the excited state of atom (having angular momentum L) by the following expressions for the photo decay $L \rightarrow L_2$.

$$P_1 = \frac{1}{I'} \begin{Bmatrix} 1 & 1 & 2 \\ L & L & L_2 \end{Bmatrix} \left(\sqrt{\frac{3}{2}} G_2(L) < T(L)^{+}_{20} > - G_2(L) < T(L)^{+}_{22} > \right), \tag{9a}$$

$$P_2 = \frac{-1}{I'} \begin{Bmatrix} 1 & 1 & 2 \\ L & L & L_2 \end{Bmatrix} \left[2\, G_2(L) < T(L)^{+}_{21} > \right], \tag{9b}$$

$$P_3 = \frac{1}{I'} \begin{Bmatrix} 1 & 1 & 1 \\ L & L & L_2 \end{Bmatrix} \left[2i\, G_1(L) < T(L)^{+}_{11} > \right], \tag{9c}$$

and

$$P_4 = \frac{1}{I'} \begin{Bmatrix} 1 & 1 & 2 \\ L & L & L_2 \end{Bmatrix} \left(\sqrt{\frac{3}{2}} G_2(L) < T(L)^{+}_{20} > + G_2(L) < T(J_b)^{+}_{22} > \right), \tag{9d}$$

where in the denominators I' and I' are :

$$I' = \frac{2(-1)^{L+L_2}}{3\sqrt{2L+1}} G_0(L) < T(L)^{+}_{00} > + \begin{Bmatrix} 1 & 1 & 2 \\ L & L & L_2 \end{Bmatrix}$$

$$\sqrt{\frac{1}{6}} G_2(L) < T(L)^{+}_{20} > + G_2(L) < T(L)^{+}_{22} > \tag{10a}$$

and

$$I' = \frac{2(-1)^{L+L_2}}{3\sqrt{2L+1}} G_0(L) < T(L)^{+}_{00} > + \begin{Bmatrix} 1 & 1 & 2 \\ L & L & L \end{Bmatrix}$$

$$\left(\sqrt{\frac{1}{6}} G_2(L) < T(L)^{+}_{20} > - G_2(L) < T(L)^{+}_{22} > \right). \tag{10b}$$

In the above eqs. (9) and (10) the curly braces denote the Wigner 6*j* symbols. $G_k(L)$ are the perturbation coefficients which take into account the fine-structure splitting and are given

$$G_K(L) = \frac{1}{(2S+1)} \sum_J (2J+1)^2 \begin{Bmatrix} L & J & S \\ J & L & K \end{Bmatrix}^2, \tag{11}$$

S is the electronic spin and $J = L + S$ is the total angular momentum of the atom. The $G_k(L)$ are normalized such that $G_0(L) = 1$ for all L. Further, the state multipoles $< T(L)^{+}_{KQ} >$ of the

excited state with orbital angular momentum L are related to the complex scattering amplitudes a_m as :

$$< T(L)^{+}_{KQ} > = \sum_{M'M} (-1)^{L-M'} \sqrt{2K+1} \begin{Bmatrix} L & L & K \\ M' & -M & -Q \end{Bmatrix} < a_{M'}\, a^{*}_{M} >. \tag{12}$$

The large round bracket is Wigner 3*j* symbol and the values of rank K and component Q of the state multipoles are restricted to K = 2L and $-K \leq Q \leq K$.

The spin average $< a_{M'}\, a^{*}_{M} >$ is defined as

$$< a_{M'}\, a^{*}_{M} > = \frac{1}{2(2S_i+1)} \sum_{S} (2S+1)\, a^{S}_{M'} a^{*S}_{M}, \tag{13}$$

where, S_i is the atomic spin in the initial state and S is the total spin of the system.

In order to characterize the excited state of the atom immediately after excitation Andersen *et al* [17] defined alignment and orientation parameters in 'natural frame of reference' which can be related to the Stokes parameter. We consider here the alignment angle γ, the linear polarization, P_l and the angular momentum transferred perpendicular to the scattering plane, $L_\perp$. These are expressed as

$$\gamma = \frac{1}{2} \tan^{-1} \left(\frac{\bar{P}_2}{\bar{P}_1} \right), \tag{14}$$

$$P_l = \sqrt{\bar{P}_1^2 + \bar{P}_2^2}\,, \tag{15}$$

and

$$L_\perp = - P_3 \left(\frac{2L}{2+k} \right), \tag{16}$$

$$k = \frac{(1+\bar{P}_1)(1-\bar{P}_4)}{(1+\bar{P}_4)}. \tag{17}$$

Here, $\bar{P}_1$ to $\bar{P}_4$ are the reduced Stokes parameters which may be obtained by using the same relations as for the measured Stokes parameters P_1, P_2, P_3 and P_4 (eqs. 9 and 10) but with all the $G_k(L)$ in their expressions taken to the unity.

3. Results and discussion

We calculated results for the various n^1P and n^3P excitations in Mg (n = 3) and Zn (n = 4) and the 3^1D and 3^3D excitations in Mg at 20 and 40 eV incident electron energies where most other calculations and experimental data are available for comparison. For all these excitations we present the DCS results and the Andersen parameters.

In Figures 1-3 our values for the DCS for Mg and Zn atoms are presented and compared. In Figure 1(a) we compare the different cross sections for the excitation of the 3^1P-state. We

have included the six-state close-coupling calculation (CC6) and the six-state close-coupling calculation which includes a continuum orbital potential (CCO6) of McCarthy *et al* [7]. Also included are the FOMBT calculations of Meneses *et al* [6] using single configuration ground state as given in tabular form in their paper. The experimental data of Brunger *et al* [18] and Williams and Trajmar [19] were reported at 10, 20 and 40 eV energies. Both sets of data are shown in the figure. For 3^1P excitation five-state CCA calculation of Mitroy and McCarthy [20] and non-relativistic DWA calculations of Clark *et al* [8] are also available. However, CCA results of Mitroy and McCarthy [20] are not included in the figure as they differ very slightly from the DCS of the CC6 calculation. We also include the single configuration ground state results of our earlier RDW calculations. From this figure, we see that all the theoretical curves have the same shape, but that there are considerable differences in magnitude, especially for larger scattering angles. On comparing our DWA values with the FOMBT results which are characterised by the feature that the distorted waves for both the incident and scattered electrons are calculated in the static-exchange potential of the ground state atom (*i.e.* similar to II model), and with the DWA results of Clark *et al* [8], who calculated the continuum wavefunction in the potential of the initial and final configurations for the incident and scattered electrons respectively (*i.e.* similar to IF model), we find that the DWA results have better agreement with the experiment than the later two theories ; especially in the forward and backward scattering angles.

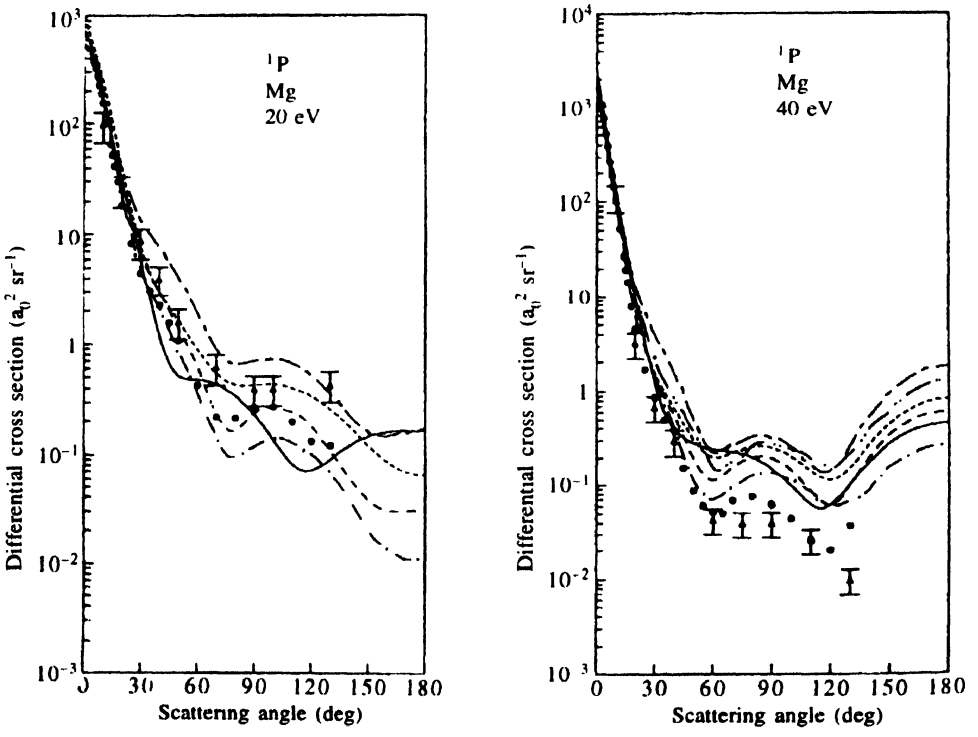

Figure 1(a). Differential cross section in units of a_0^2 sr^{-1} for electron impact excitation of the 3^1P state of magnesium at 20 and 40 eV. _____, Present DWA results ; — - —, RDW results ; - - - - -, FOMBT results ; - - - -, CC6 results ; — . —, CCO6 results ; — .. —, DWA results of Clark *et al* [8]. Experiment, •, Brunger *et al* [18] ; Δ, Williams and Trajmar [19].

In Figure 1(b) we compare the different cross sections for the excitation of the 3^3P-state. The only difference to Figure 1(a) is that the experimental DCS data are now taken from the improved experimental data of Houghton *et al* [21] available only at 10 and 20 eV. On comparing our DWA results with the FOMBT results we find that the comparison of the DWA results is better in the forward scattering angle range $0\text{-}40^0$ while FOMBT does better in the range $50\text{-}120^0$. No conclusion for the most suitability of a particular approximation method can hence be drawn from Figures 1(a) and 1(b). In both these figures we find the best overall agreement can be said for the CCA results.

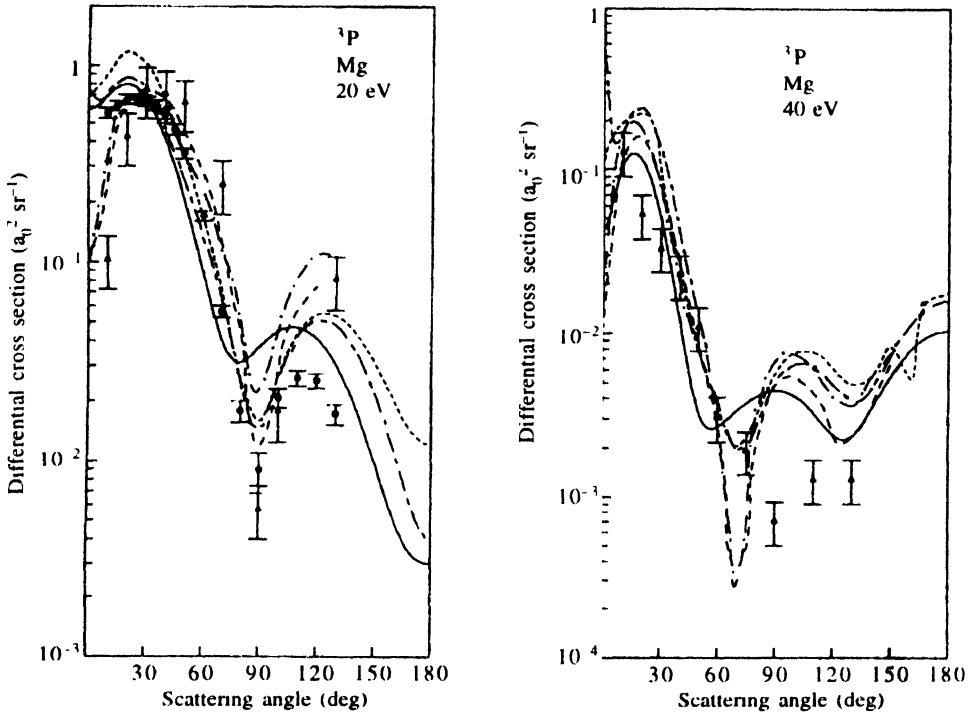

Figure 1(b). Same as Figure 1(a) but for 3^3P state of magnesium at 20 eV and 40 eV Theory . as in Figure 1(a). Experiment, •, Houghton *et al* [21].

In Figure 2 we compare our DWA results with our earlier RDW results for $3^{1,3}D$ excitations in magnesium. Williams and Trajmar [19] reported data at 10,20 and 40 eV energies for the 3^1D excitation as well as for the unresolved $3^3D + 4^3P$ states. We have included only their data for the 3^1D excitation for comparison in Figure 2 as our results for 3^3D excitation cannot be directly compared with the experiment. The measured DCS results for the 3^1D_2-state are relative and William and Trajmar [19] used the same normalization as for the excitation of the $3^{1,3}P$ states. This experiment when normalized with respect to the RDW or the DWA results shows good comparison with the normalized curve. There is qualitative agreement with both the results. However, we find that though for ^1D results the comparison between the RDW and DWA results is not very convincing, but for ^3D results the similar structures for both RDW and DWA are encouraging.

Finally in Figure 3, we present an inter-comparison of the RDW and DWA results for the $4^{1,3}P$ excitations in Zn for which there are no other experimental or theoretical data. For 4^1P

transition in zinc as expected we find that with the increase in energy the agreement between the RDW and DWA calculation improves. Further for 4^3P excitation we find that there is a qualitative agreement between the RDW and DWA calculations. Also, with the increase in energy more structures are seen in both the RDW and DWA results. Note that in LS-coupling the 4^3P excitation from the ground 4^1S state can occur only through an electron spin-exchange process, but in a relativistic treatment spin-flip can occur via spin-orbit coupling as well. In order to draw more meaningful comparisons for the $4^1S \rightarrow 4^{1,3}P$ excitations in Zn, more theoretical and experimental work should be taken up.

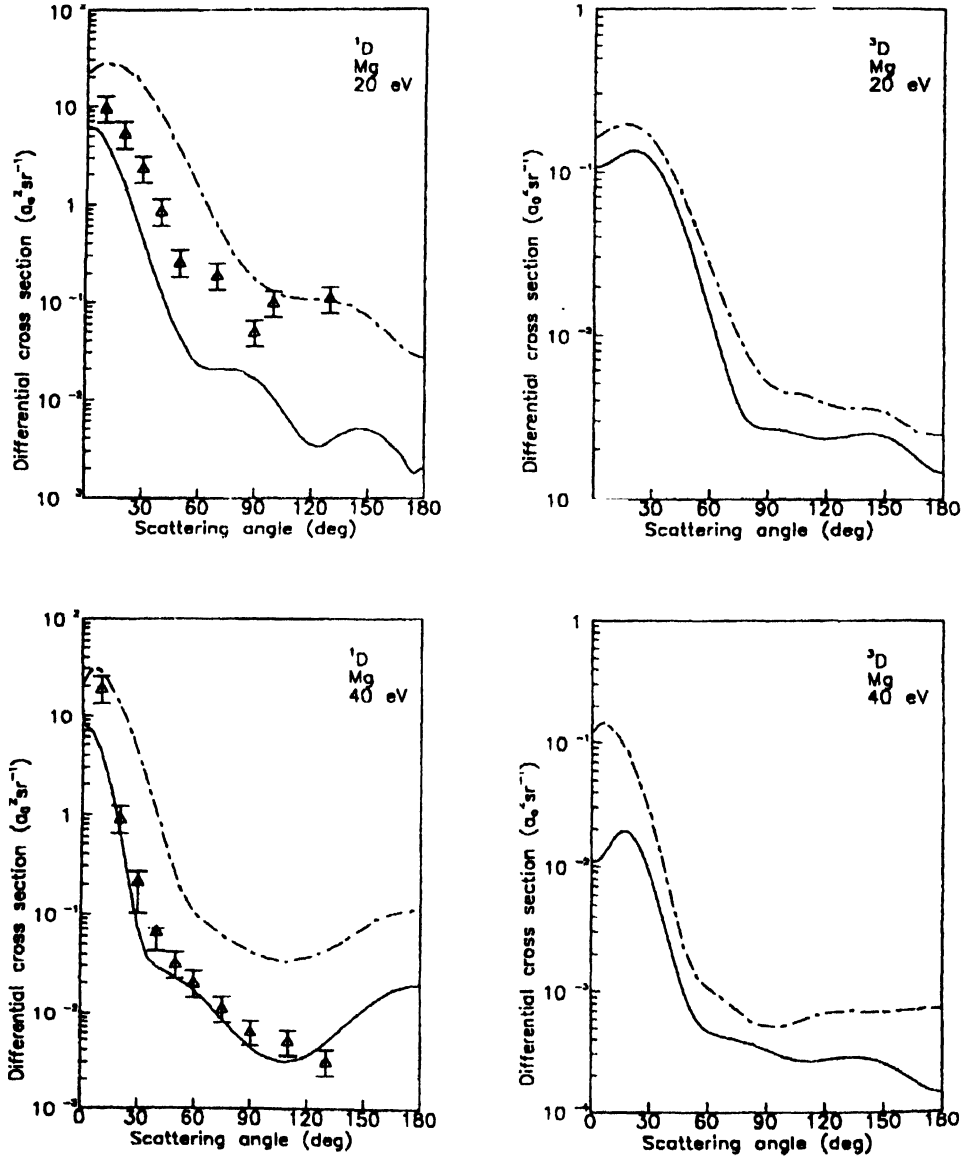

Figure 2. Differential cross section in units of a_0^2 sr^{-1} for electron impact excitation of the 3^1D and 3^3D states of magnesium at 20 and 40 eV _____ , Present DWA results ; — - — , RDW results. Experiment, Δ, Williams and Trajmar [19].

In Figure 4(a), we show the orientation and alignment parameters P_l, γ and $L_\perp$ respectively for the 3^1P and 3^3P excitations in magnesium at 40 eV. In these figures, we have compared our DWA and RDW results with the DWA results of Clark *et al* [8] and the FOMBT calculations of

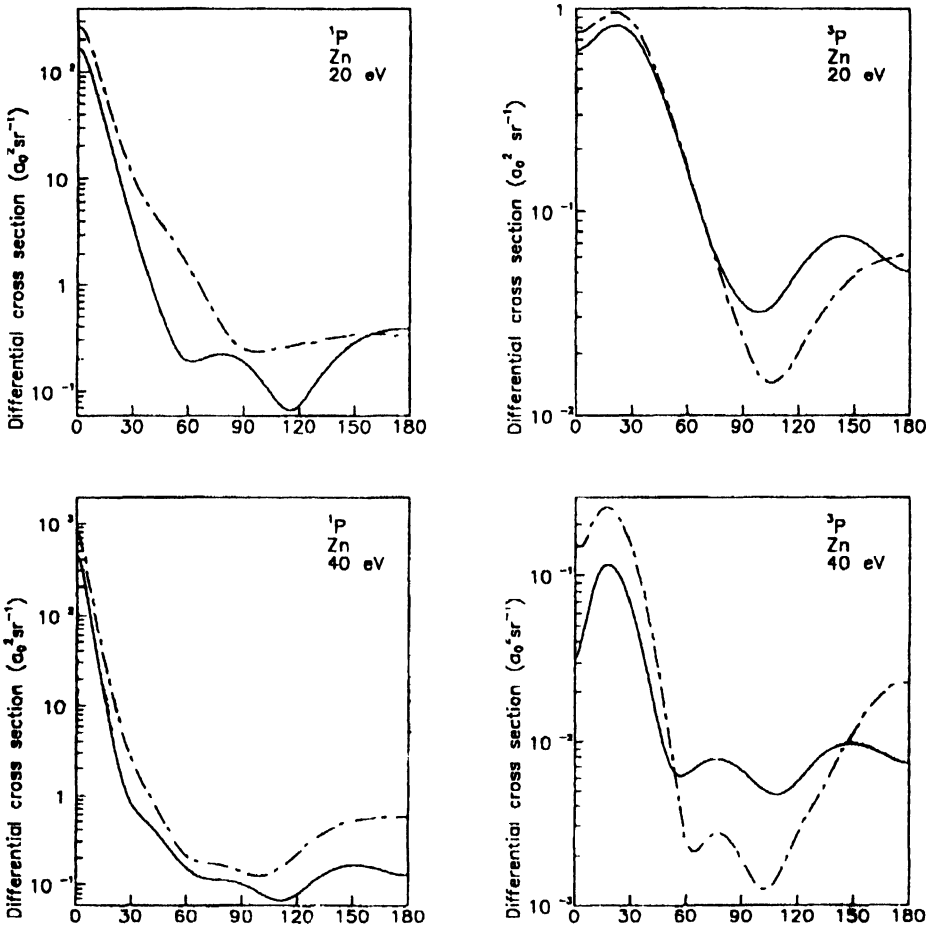

Figure 3. Same as Figure 2 but for 4^1P and 4^1P states of zinc at 20 and 40 eV

Meneses *et al* [6] for 3^1P excitation in magnesium. For 3^3P excitation in magnesium we compare DWA and RDW results with the FOMBT results of Meneses *et al* [6]. Experimental results have been reported by Brunger *et al* [18] only for the 3^1P excitation in the limited angular range of $5\text{-}20^0$ for 20 and 40 eV incident electron energies. Mitroy and McCarthy [20] have also given five-state CCA results for the 3^1P state in the angular range for the incident energies where the experimental data exist. Since their results are in very good agreement with our earlier RDW results and the FOMBT results, for sake of clarity these are not shown. In Figure 4(a) we see that though all the theories agree well with the available experimental data of Brunger *et al* [18] for 3^1P excitations in Mg, the DWA results are far away from the experiment. All the curves show similar structures. As we can clearly see here, these parameters are very sensitive to the distortion potential used.

In Figure 4(b) we inter-compare our DWA results with the earlier reported RDW results for the 4^1P and 4^3P excitations in Zn at 20 eV. Peak to peak structures are not followed and the

two theories differ in magnitude also. It would be highly desirable to have experimental data to provide a more extensive test of the theoretical models.

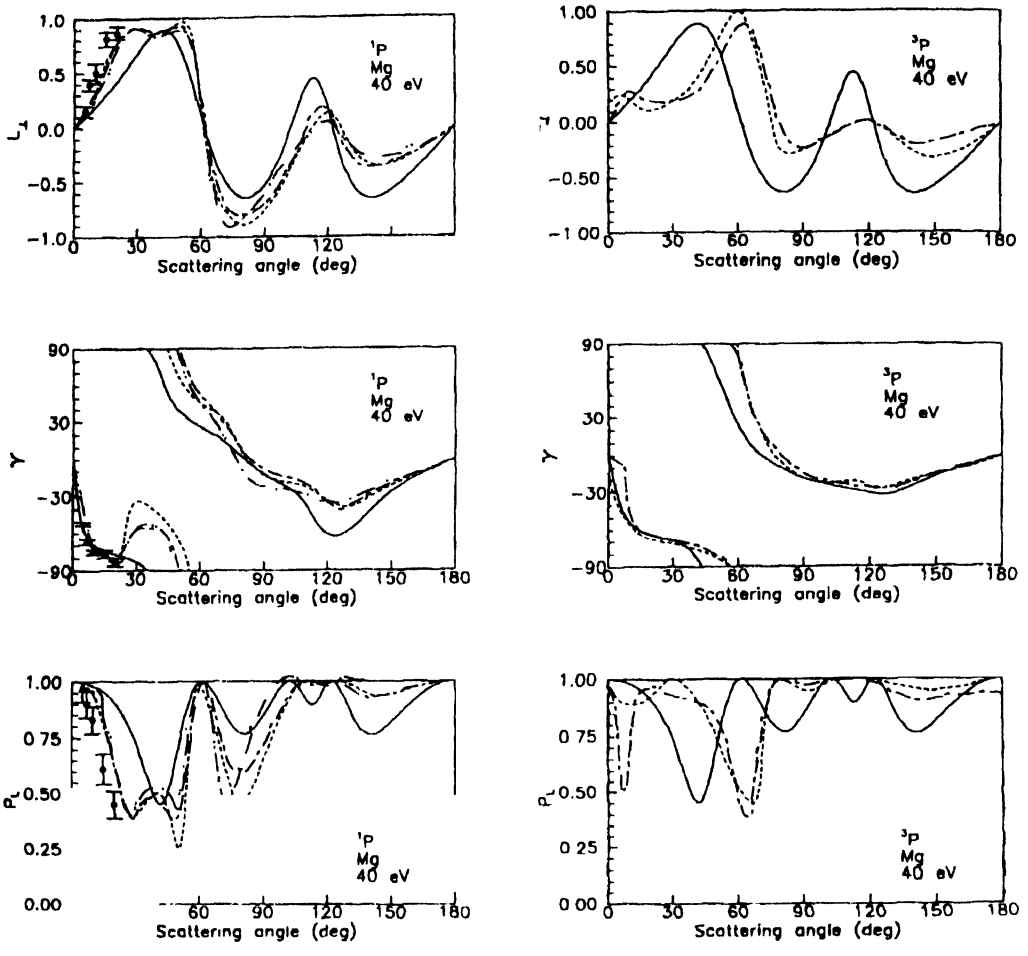

Figure 4(a). The parameters L_1, P_l and γ for the electron impact of the 3^1P and 3^3P states of magnesium at 40 eV _____, Present DWA results, — — —, RDW results, - - - - -, FOMBT results, · · — DWA results of Clark *et al*[8] Experiment, ●, Brunger *et al* [18]

4. Conclusion

We have presented our distorted-wave approximation calculations for the differential cross section, coherence and correlation parameters for electron impact excitation of the $3^{1,3}$P and $3^{1,3}$D states of magnesium and $4^{1,3}$P states of zinc from their respective ground 3^1S_0 and 4^1S_0 states. The agreement of our DWA results for the $3^{1,3}$P excitations in Mg are similar to those reported earlier in literature. However, our earlier RDW results differ from the present DWA results. In case of $4^{1,3}$P excitations in zinc and at high energy the RDW and DWA results compare well. Further, we find that for the 3^1D_2 results in magnesium the DWA results show better agreement with the experiment as compared to the RDW results. The difference in our RDW and DWA results could arise due to different wavefunctions used and also due to the

difference in the way exchange has been treated in both the approximations. Finally, more experimental and theoretical studies are needed to enable us to draw a better conclusions.

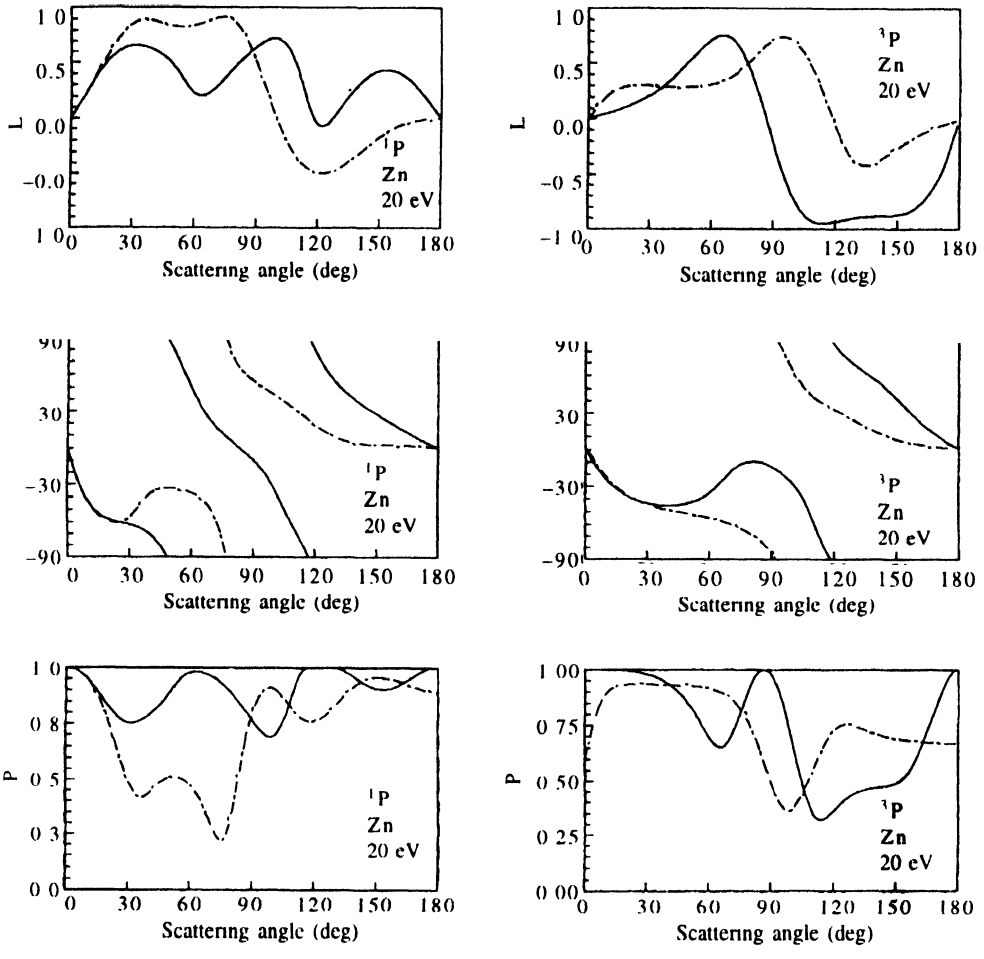

Figure 4(b). The parameters L_1, P_1 and γ for the electron impact of the 4^1P and 4^3P states of Zinc at 20 eV. _____, Present DWA results, — - — , RDW results.

Acknowledgment

We are grateful to the New Computational Facilities (NCF) at the University of Roorkee, for permission to use their computer. The author (RS) is thankful to the University Grants Commission (UGC), New Delhi and the authors (SK and SV) are thankful to the Council of Scientific and Industrial Research (CSIR), New Delhi for the financial assistance to this work.

References

[1] B Markinkovic, V Pejcev, D Fillipovic and L Vuskovic *J. Phys.* **B24** 1817 (1991)

[2] P W Zetner, Y Li and S Trajmar *J. Phys.* **B25** 3187 (1992) ; **48** 495 (1993)

[3] Y Li and P W Zetner *Phys. Rev.* **A49** 950 (1994)

[4] H J Beyer, H Hamdy, E I M Zohny, K R Mohoud, M A K El-Fayoumi, H Kleinpopeen, Jr Abdallah, R E H Clark and G Csanak. *Z Phys.* **D30** 91 (1994)

[5] M R Law and P J O Teubner *J. Phys* **B28** 2257 (1995)

[6] G D Meneses, C B Pagan and L E Machado *Phys. Rev.* **A41** 4740 (1990)

[7] I E McCarthy, K Ratnavelu and Y Zhou *J. Phys* **B22** 2597 (1989)

[8] R E H Clark, G Csanak and J Abdullah Jr *Phys. Rev.* **A44** 2874 (1991)

[9] S Kaur, R Srivastava, R P McEachran and A D Stauffer *J. Phys* **B30** 1027 (1997)

[10] J B Furness and I E McCarthy *J. Phys* **B6** 2280 (1973)

[11] S Vucic, R M Potvliege and C J Joachain *J. Phys* **B20** 3157 (1987)

[12] D H Madison, K Bartschat and R Srivastava *J. Phys* **B24** 1839 (1991)

[13] N F Mott and H S W Massey *The Theory of Atomic Collisions*, (London . Oxford University Press) (1965)

[14] D H Madison and K Bartschat *Computational Atomic Physics : Electron and Positron Collisions with Atoms and Ions*, ed K Bartschat (Berlin, Heidelberg Springer-Verlag) p 65 (1996)

[15] C Froesce Fischer *Comput. Phys. Commun* **1** 151 (1969)

[16] K Blum *Density Matrix Theory and Applications*, (New York Plenum) (1981)

[17] N Andersen, J W Gallagher and I V Hertel *Phys. Rep* **165** 1 (1988)

[18] M J Brunger, J L Riley, R E Scholten and P J O Teubner *J. Phys* **B21** 1639 (1988) , **22** 1431 (1989)

[19] W Williams and S Trajmar *J. Phys* **B11** 2021 (1978)

[20] J Mitroy and I E McCarthy *J. Phys* **B22** 641 (1989)

[21] R K Houghton, M J Brunger, G Shen and P J O Teubner *J. Phys* **B27** 3573 (1994)